Nowaczyk, N., Antonow, M., Knies, J., Spielhagen, R. F. (2003): Further rock magnetic and chronostratigraphic results on reversal excursions during the last 50 ka as derived from northern high latitudes and discrepancies in precise AMS 14C dating. - Geophysical Journal International, 155, 3, pp. 1065—1080.

DOI: http://doi.org/10.1111/j.1365-246X.2003.02115.x

*Geophys. J. Int.* (2003) **155,** 1065–1080

# Further rock magnetic and chronostratigraphic results on reversal excursions during the last 50 ka as derived from northern high latitudes and discrepancies in precise AMS $^{14}$C dating

Norbert R. Nowaczyk,[1] Martin Antonow,[2,*] Jochen Knies[3,†] and Robert F. Spielhagen[2]

[1] *GeoForschungsZentrum Potsdam, Projektbereich* 3.3, *Telegrafenberg Haus C,* 14473 *Potsdam, Germany. E-mail: nowa@gfz-potsdam.de*
[2] *GEOMAR, Wischhofstraße* 1–3, 24148 *Kiel, Germany.*
[3] *Alfred-Wegener-Institute for Polar and Marine Research, Columbusstrasse,* 27568 *Bremerhaven, Germany*

Accepted 2003 August 25. Received 2003 August 25; in original form 2001 September 5

## SUMMARY

A total of five sediment cores from three sites, the Arctic Ocean, the Fram Strait and the Greenland Sea, yielded evidence for geomagnetic reversal excursions and associated strong lows in relative palaeointensity during oxygen isotope stages 2 and 3. A general similarity of the obtained relative palaeointensity curves to reference data can be observed. However, in the very detail, results from this high-resolution study differ from published records in a way that the prominent Laschamp excursion is clearly characterized by a significant field recovery when reaching the steepest negative inclinations, whereas only the N–R and R–N transitions are associated with the lowest values. Two subsequent excursions also reach nearly reversed inclinations but without any field recovery at that state. A total of 41 accelerator mass spectrometry (AMS) $^{14}$C ages appeared to allow a better age determination of these three directional excursions and related relative palaeointensity variations. However, although the three sites yielded more or less consistent chronological as well as palaeomagnetic results a comparison to another site, PS2644 in the Iceland Sea, revealed significant divergences in the ages of the geomagnetic field excursions of up to 4 ka even on basis of uncalibrated AMS $^{14}$C ages. This shift to older $^{14}$C ages cannot be explained by a time-transgressive character of the excursions, because the distance between the sites is small when compared with the size of and the distance to the geodynamo in the Earth's outer core. The most likely explanation is a difference of reservoir ages and/or mixing with old $^{14}$C-depleted $CO_2$ from glacier ice expelled from Greenland at site PS2644.

**Key words:** AMS $^{14}$C dating, geomagnetic reversals, magnetostratigraphy, palaeointensity, reversal excursions.

## INTRODUCTION

Numerous magnetostratigraphic investigations on Arctic marine sediments have yielded detailed records of several geomagnetic reversal excursions during the Brunhes Chron, especially for the time interval of the last approximately 100 ka (Løvlie *et al.* 1986; Bleil 1989; Bleil & Gard 1989; Nowaczyk & Baumann 1992; Nowaczyk *et al.* 1994; Schneider *et al.* 1996; Nowaczyk 1997; Nowaczyk & Antonow 1997; Voelker *et al.* 1998; Nowaczyk & Frederichs 1999; Knies *et al.* 2000; Laj *et al.* 2000; Nowaczyk & Knies 2000). One of the best documented excursion now is the Laschamp reversal excursion at around 40 ka, calibrated BP, originally found in volcanics of the Massif Centrale in France (Bonhommet & Babkine 1967; Gillot *et al.* 1979) and later also in sediments of Lac St Front (Vlag *et al.* 1996) as well as in volcanics on Iceland (Levi *et al.* 1990) and probably Hawaii (Laj *et al.* 2002).

In the Arctic realm, however, because of the widespread absence of foraminifers in the water column for certain, often long time intervals, precise dating of the respective sediments generally are difficult to obtain. Only at some individual sites presented in this paper could a sufficient amount of foraminifers be collected throughout major sections of the cores in order to establish accelerator mass spectrometry (AMS) $^{14}$C chronologies. Magnetostratigraphic investigation on three cores from northern high latitudes Fig. 1), PS2138-1 (81.5°N, Eastern Arctic Ocean Nowaczyk & Knies 2000), PS1535-8 (78.7°N, Fram Strait, Nowaczyk & Baumann 1992) and PS1878-3 (73.3°N, Greenland Basin, Nowaczyk 1997; Nowaczyk & Antonow 1997), yielded records of several short-term geomagnetic reversal excursions, with the Laschamp excursion being the most

*Now at: Museum für Naturkunde, Theaterplatz 1, 09111 Chemnitz, Germany.
†Now at: Geological Survey of Norway, 7491 Trondheim, Norway.

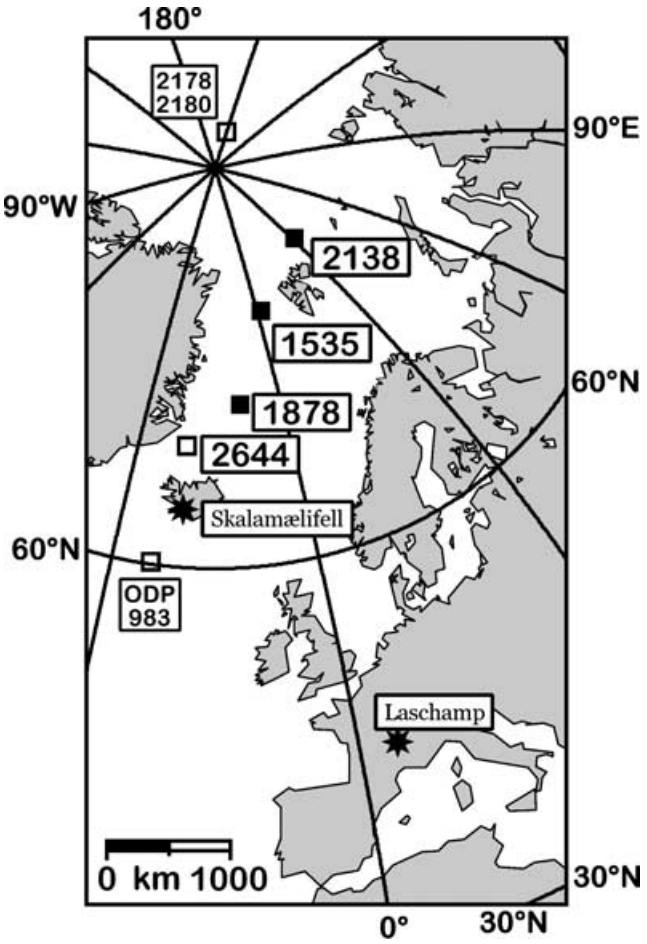


**Figure 1.** Location map of investigated sites. Closed squares, cores presented in this paper; open squares, cores 2178/2180: Nowaczyk *et al.* (2001), core 2644: Voelker *et al.* (1998), ODP site 983: Channell *et al.* (1997). Asterisks denote documentations of the Laschamp excursion in volcanic rocks: Laschamp (France), Bonhommet & Babkine (1967), Gillot *et al.* (1979); Skalamælifell (Iceland), Levi *et al.* (1990).

pronounced one. In all three cores the Laschamp excursion is documented in a depth interval of approximately 25–45 cm thickness, but with significantly different thicknesses of overlying sediments. In particular, the first record published from Fram Strait suggested a very long duration of 9 ka (34–43 ka) of the Laschamp excursion when using the rough age estimate of Nowaczyk & Baumann (1992) which was based on calcareous nanofossil and oxygen isotope stratigraphies and the assumption of a continuous sedimentation. Since publication of the palaeomagnetic results large efforts have been made in order to evaluate absolute ages for the investigated cores. Beside 11 already published results on AMS $^{14}$C dating (10 on PS2138-1 and 1 on PS1878-3) we present here further detailed rock magnetic analyses and 33 new AMS $^{14}$C ages (see Table 2 below) yielding more detailed information concerning the timing of the geomagnetic field variation documented within the magnetizations of the cores, especially geomagnetic excursions and related relative palaeointensity variations.

## MATERIAL AND METHODS

Palaeomagnetic and rock magnetic investigations on core PS2138-1, eastern Arctic Ocean, cores PS1535-8 and -10, Fram Strait, and core PS1878-1, Greenland Basin, have been published in some detail as referenced in Table 1. Core PS1535-6, Fram Strait, was chosen for this paper in order to investigate the palaeomagnetism and rock magnetism of Fram Strait sediments in more detail. Following the techniques described by, for example, Nowaczyk & Baumann (1992), Nowaczyk & Antonow (1997) and Nowaczyk & Knies (2000), the samples were subjected to progressive alternating field demagnetization of the natural remnant magnetization (NRM) with subsequent vectorial analysis by principal component analysis (Kirschvink 1980), and acquisition/demagnetization experiments of anhysteretic and isothermal remnant magnetization (ARM and IRM). ARMs were produced with 100 mT alternating field (AF) amplitude and a static field of 50 μT. IRMs acquired at 1.5 T are referred to as saturated IRM (SIRM). For determination of the *S*-ratio the samples were subjected after SIRM acquisition to a field of 0.3 T in the opposite direction. In order to exclude the theoretical possibility that non-normal palaeomagnetic directions are associated with an anomalous (magnetic) fabric, the samples from core PS1535-6 were also used for analysis of the anisotropy of magnetic susceptibility using an AGICO KLY-3S Kappabridge, that is, susceptibility is measured numerous times while the sample is rotating around the *x*-, *y*- and *z*-axes, respectively. Measurements from the three orthogonal planes are combined with one bulk measurement in order to calculate the complete anisotropy tensor (with AGICO software), represented by the general susceptibilities $K_{max}$, (maximum), $K_{int}$ (intermediate) and $K_{min}$ (minimum), and their respective orientation angles, declination and inclination. The orientation angles are given with respect to sample coordinates because the azimuth of the core is unknown.

17 samples from the lower section of core PS1878-3, 10 samples from the upper section of PS1535-6 and 40 samples more or less equally distributed along the core axis of core PS2138-1 were used for low-temperature measurements of magnetic susceptibility using the CS-L furnace of the KLY-3 Kappabridge in order to provide further information concerning the mineralogy of the remanence carriers for all three investigated sites. After subtracting the furnace background the ferrimagnetic susceptibility was separated from the paramagnetic contribution by subtracting a hyperbola from the furnace-corrected data using the CUREVAL 5.0 program supplied with the Kappabridge. The hyperbola was fitted between −140 and −70 °C (see also Nowaczyk *et al.* 2002).

**Table 1.** Locations of sediment cores from north to south. References for palaeomagnetic results are: (1) Nowaczyk & Knies (2000), (2) Nowaczyk & Baumann (1992), (3) Nowaczyk (1997), (4) Nowaczyk & Antonow (1997).

| Core number | Latitude | Longitude | Water depth | Length | Area | Reference |
|---|---|---|---|---|---|---|
| PS2138-1 | 81° 32.1′ N | 30° 35.6′ E | 995 m | 635 cm | Eastern Arctic Ocean | (1) |
| PS1535-6 | 78° 45.4′ N | 1° 49.5′ E | 2555 m | 390 cm | Fram strait | This study |
| PS1535-8 | 78° 44.8′ N | 1° 52.8′ E | 2557 m | 496 cm | Fram strait | (2) |
| PS1535-10 | 78° 43.6′ N | 1° 57.0′ E | 2554 m | 814 cm | Fram strait | (2) |
| PS1878-3 | 73° 15.3′ N | 9° 00.7′ W | 3048 m | 469 cm | Greenland Basin | (3), (4) |

**Table 2.** AMS $^{14}$C and calibrated ages from cores discussed in this paper. (1) Knies *et al.* (2000); (2) Nowaczyk & Antonow (1997); (3) mean value of CALIB4.3 program results. N.p. *Neogloboquadrina pachyderma* (sin.); b.F., benthic forams; P., *Pyrgo*.

| Core | Depth (cm) | AMS $^{14}$C Age (ka) | 440 yr reservoir corrected (ka) | Calibrated age (ka, BP) | Material | Reference |
|---|---|---|---|---|---|---|
| PS 2138-1 | 50 | 13.46 ± 0.11 | 13.02 | 15.55 | | (1) |
| PS 2138-1 | 65 | 13.43 ± 0.07 | 12.99 | 15.52 | N.p. | This study |
| PS 2138-1 | 80 | 13.04 ± 0.14 | 12.60 | 14.73[3)] | | (1) |
| PS 2138-1 | 110 | 14.03 ± 0.08 | 13.59 | 16.21 | | (1) |
| PS 2138-1 | 130 | 15.85 ± 0.13 | 15.41 | 18.30 | | (1) |
| PS 2138-1 | 160 | 16.67 ± 0.21 | 16.23 | 19.24 | | (1) |
| PS 2138-1 | 200 | 17.32 ± 0.13 | 16.88 | 19.99 | | (1) |
| PS 2138-1 | 230 | 19.23 ± 0.14 | 18.79 | 22.19 | N.p. | This study |
| PS 2138-1 | 244 | 19.71 ± 0.13 | 19.27 | 22.74 | N.p. | This study |
| PS 2138-1 | 260 | 20.42 ± 0.13 | 19.98 | 23.56 | N.p. | This study |
| PS 2138-1 | 275 | 20.70 ± 0.13 | 20.26 | 23.88 | N.p. | This study |
| PS 2138-1 | 300 | 20.48 ± 0.33 | 20.04 | 23.63 | | (1) |
| PS 2138-1 | 316 | 22.47 ± 0.16 | 22.03 | 25.83 | N.p. | This study |
| PS 2138-1 | 331 | 23.54 ± 0.24 | 23.10 | 26.98 | | (1) |
| PS 2138-1 | 345 | 24.91 ± 0.20 | 24.47 | 28.47 | N.p. | This study |
| PS 2138-1 | 360 | 26.24 ± 0.28 | 25.80 | 29.88 | | (1) |
| PS 2138-1 | 366 | 26.26 ± 0.23 | 25.82 | 29.90 | N.p. | This study |
| PS 2138-1 | 372 | 30.29 ± 0.36 | 29.85 | 33.65 | b.F., N.p. | This study |
| PS 2138-1 | 375 | >45.19 | | >46.55 | b.F., N.p. P | This study |
| PS 2138-1 | 380 | 35.34 ± 1.57 | 34.90 | 38.50 | | (1) |
| PS 2138-1 | 382 | 29.62 ± 0.20 | 29.18 | 33.10 | N.p. | This study |
| PS 2138-1 | (a) 385 | 30.24 ± 0.38 | 29.80 | 33.60 | N.p. | This study |
| PS 2138-1 | (b) 385 | 30.81 ± 0.21 | 30.37 | 34.13 | N.p. | This study |
| PS 2138-1 | 387 | 31.67 ± 0.24 | 31.23 | 34.87 | N.p. | This study |
| PS 1535-8 | 35 | 16.65 ± 0.17 | 16.21 | 19.22 | N.p. | This study |
| PS 1535-8 | 45 | 18.15 ± 0.25 | 17.71 | 20.95 | N.p. | This study |
| PS 1535-8 | 55.5 | 19.05 ± 0.17 | 18.61 | 21.98 | N.p. | This study |
| PS 1535-8 | 61.5 | 20.62 ± 0.19 | 20.18 | 23.79 | N.p. | This study |
| PS 1535-8 | 75 | 24.55 ± 0.30 | 24.11 | 28.07 | N.p. | This study |
| PS 1535-8 | 83.5 | 29.34 ± 0.41 | 28.90 | 32.86 | N.p. | This study |
| PS 1535-8 | 89 | 29.80 ± 0.28 | 29.36 | 33.24 | N.p. | This study |
| PS 1535-8 | 97 | 31.90 ± 0.26 | 31.46 | 35.10 | N.p. | This study |
| PS 1535-8 | 109 | 33.45 ± 0.45 | 33.01 | 36.65 | N.p. | This study |
| PS 1878-3 | 100 | 16.44 ± 0.12 | 16.00 | 18.98 | N.p. | This study |
| PS 1878-3 | 145 | 19.37 ± 0.15 | 18.93 | 22.35 | N.p. | This study |
| PS 1878-3 | 250 | 24.21 ± 0.15 | 23.77 | 27.69 | N.p. | This study |
| PS 1878-3 | 270 | 28.35 ± 0.19 | 27.91 | 31.95 | N.p. | This study |
| PS 1878-3 | 280 | 28.53 ± 0.33 | 28.09 | 32.13 | N.p. | (2) |
| PS 1878-3 | 300 | 28.63 ± 0.18 | 28.19 | 32.23 | N.p. | This study |
| PS 1878-3 | 340 | 30.90 ± 0.49 | 30.46 | 34.14 | N.p. | This study |
| PS 1878-3 | 370 | 23.47 ± 0.22 | 23.04 | 26.92 | N.p. | This study |
| PS 1878-3 | 380 | 30.74 ± 0.23 | 30.30 | 34.06 | N.p. | This study |
| PS 1878-3 | 390 | 33.78 ± 0.67 | 33.34 | 36.98 | N.p. | This study |
| PS 1878-3 | 410 | 40.80 ± 0.65 | 40.36 | 43.36 | N.p. | This study |

In general, 1200–1600 specimens of the planktic foraminifera *Neogloboquadrina pachyderma* sin. were selected from the 125–250 μm grain size fraction for each sample for the AMS $^{14}$C measurements. Partly, other forms were used, as indicated in Table 2. All dating were performed at the AMS facility of the *Leibniz–Labor für Altersbestimmung und Isotopenforschung* of the *Christian-Albrechts-Universität Kiel*, Germany. Radiocarbon ages <20.3 ka were calibrated by the CALIB4.3 program (Stuiver & Reimer 1993) with the data set from Stuiver *et al.* (1998). For radiocarbon ages >20.3 kyr, age shifts were obtained from Voelker *et al.* (1998). At 20.3 ka, the offset of both methods is <200 yr.

## RESULTS

### Palaeomagnetism

Fig. 2 compiles vector endpoint diagrams of a total of 13 samples from sediments deposited during the Laschamp excursion at the three sites discussed in this paper. The clearly upward directed ChRM directions are all superimposed by a more or less large downward directed overprint, that is, a viscous component parallel to the recent field. This overprint persists until demagnetization amplitudes of 35–50 mT. Therefore, for samples such as in Fig. 2, demagnetization results below this level were not included in the

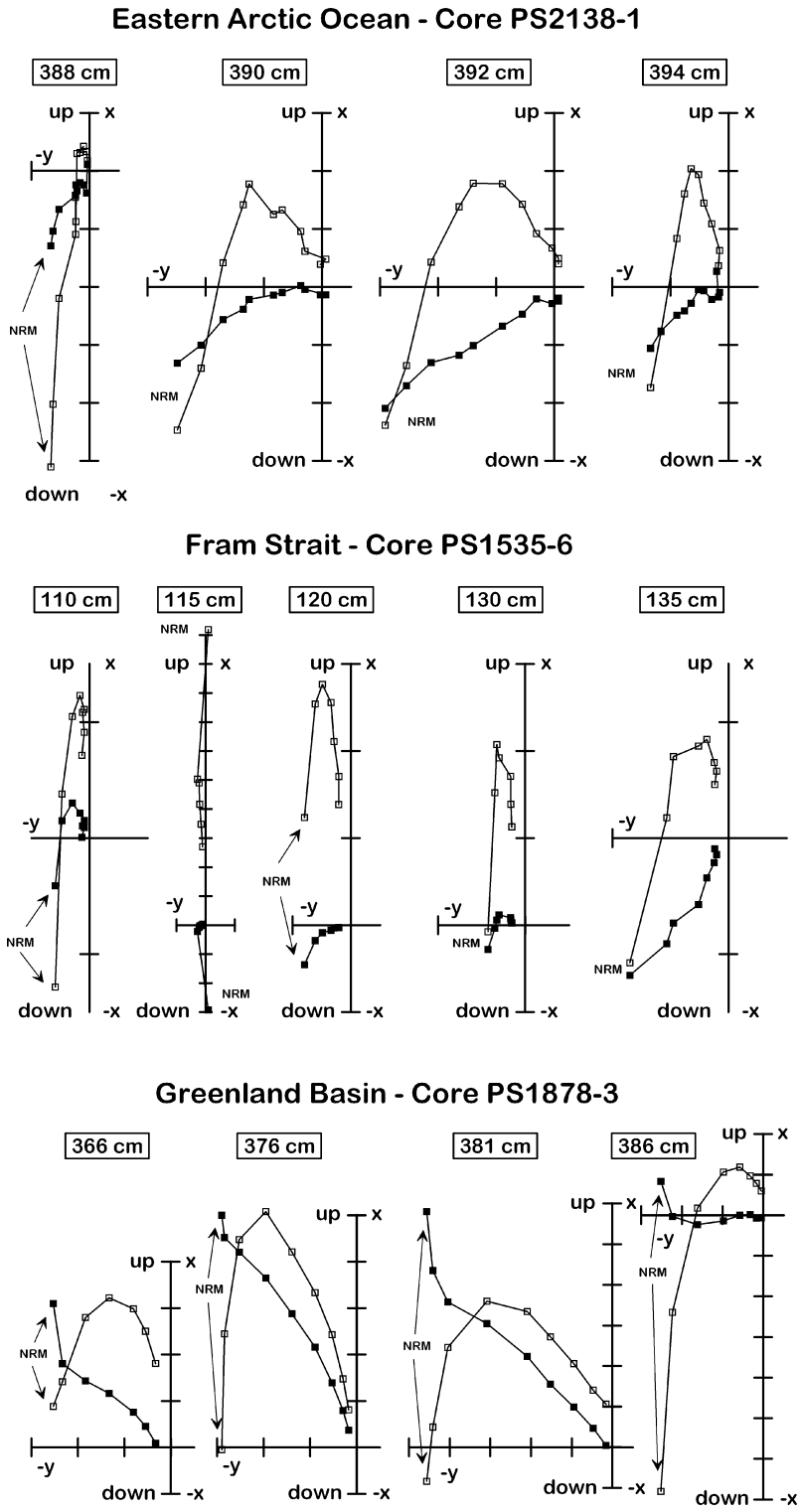


**Figure 2.** Orthogonal projections, vector endpoint diagrams, of demagnetization results from cores PS1878-3, PS1535-6 and PS2138-1. Sediments related to the 13 samples were deposited during the Laschamp reversal excursion. Solid (open) symbols denote the horizontal (vertical) plane. Demagnetization steps are 0, [5], 10, [15], 20, 35, 50, 65, 80, [95 or 100] mT. The tick spacing is equivalent to 1.0 mA $m^{-1}$.

determination of ChRM directions. Down-core plots of ChRM inclinations of all three cores are presented in Figs 3(a) and (b), showing the pronounced Laschamp reversal excursion (indicated by 'La') in all three cores. Where present, oxygen isotope stage 5 is marked by horizontal dashed lines and the ages of the core bases are also indicated, according to the respective age models (PS1878-3: Nowaczyk & Antonow 1997; PS1535-8, parallel to PS1535-6: Nowaczyk & Baumann 1992; Matthiessen *et al.* 2001; PS2138-1: Nowaczyk & Knies 2000; Matthiessen *et al.* 2001). It is interesting to note that the Laschamp excursion is documented in all three cores within an interval of 25–45 cm thickness but with a highly variable thickness for the overlying sediments that were deposited

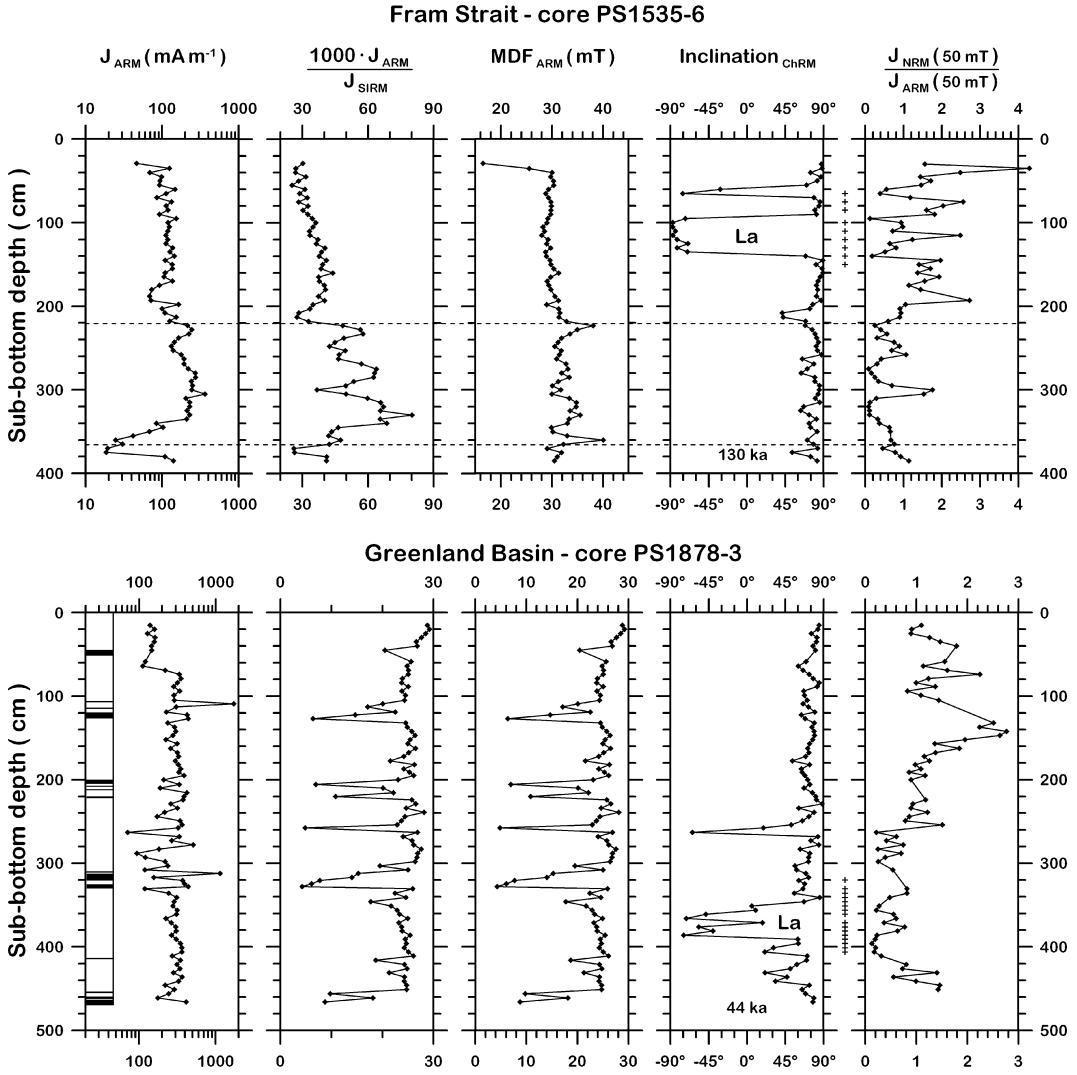


**Figure 3.** (a) Rock and palaeomagnetic data from cores PS1878-3 and PS1535-6: down-core variations of parameters related to magnetic concentration, magnetic grain size and coercivity together with inclinations of characteristic remnant magnetization ($\text{Incl}_{\text{ChRM}}$) and palaeointensity estimate. $J_{\text{ARM}}$, intensity of anhysteretic remnant magnetization ($B_{\text{stat}} = 50\ \mu\text{T}$, $B_{\text{AF}} = 100$ mT); $J_{\text{SIRM}}$, intensity of saturated isothermal remnant magnetization ($B = 1.5$ T); $\text{MDF}_{\text{ARM}}$, median destructive field of ARM. Crosses indicate positions of samples used for low-temperature measurements of magnetic susceptibility (see Fig. 7). (b) Rock and palaeomagnetic data from core PS2138-1.

during the last approximately 40 ka. Their thicknesses range from 380 cm (PS2138-1, Laschamp: 25 cm) to only 95 cm (PS1535-6, Laschamp: 45 cm). At two coring sites further north, at 88°N and 155°E (PS2178 and PS2180, Fig. 1), an approximately 30 cm thick layer documenting the Laschamp excursion is covered by only 40 cm of sediments (Nowaczyk *et al.* 2001). The fairly constant thickness of the Laschamp excursion in an area spanning from the Greenland Sea to the central Arctic Ocean, on the one hand, and the extreme differences in the overlying sediments, on the other hand, in general, indicate a highly variable sedimentation both in time and space within the Arctic, but a high deposition rate with little spatial variability contemporary to the Laschamp excursion. This gives a quite interesting palaeoceanographic as well as palaeoclimatic aspect, but this shall not be the main topic of this paper.

## Rock magnetism

Some basic rock magnetic parameters, the intensity of anhysteretic remnant magnetization ($J_{\text{ARM}}$), the ratio of $J_{\text{ARM}}$ to the intensity of saturated isothermal remnant magnetization ($J_{\text{SIRM}}$), and the median destructive field of the ARM ($\text{MDF}_{\text{ARM}}$) are also displayed in Figs 3(a) and (b). Variations in concentration of magnetic minerals as measured by ARM intensities ($J_{\text{ARM}}$) are in the range of an order of magnitude in all three cores. Ratios of ARM intensity to SIRM intensity ($J_{\text{ARM}}/J_{\text{SIRM}}$), as estimates of magnetic grain size and median destructive fields of ARM ($\text{MDF}_{\text{ARM}}$), as a measure of coercivity, are fairly constant in the upper half of core PS1535-6, but with a higher variability and a general trend to more fine-grained material in the lower half of the core (oxygen isotope stage 5). In core PS1878-3 ARM/SIRM ratios $\text{MDF}_{\text{ARM}}$ values are also quite constant but with tephra layers (see the lithology column in Fig. 3a) showing significantly lower ARM/SIRM ratios and $\text{MDF}_{\text{ARM}}$, respectively. Core PS2138-1 is also characterized by quite constant magnetic concentration and grain size parameters, except for the Holocene in the top and stage 5 sediments near the bottom, which both deviate from the general trend with generally higher ARM/SIRM ratios and higher $\text{MDF}_{\text{ARM}}$ values. Further rock magnetic data for core PS1878-3 are given in Nowaczyk (1997) and for core PS2138-1 in Nowaczyk &

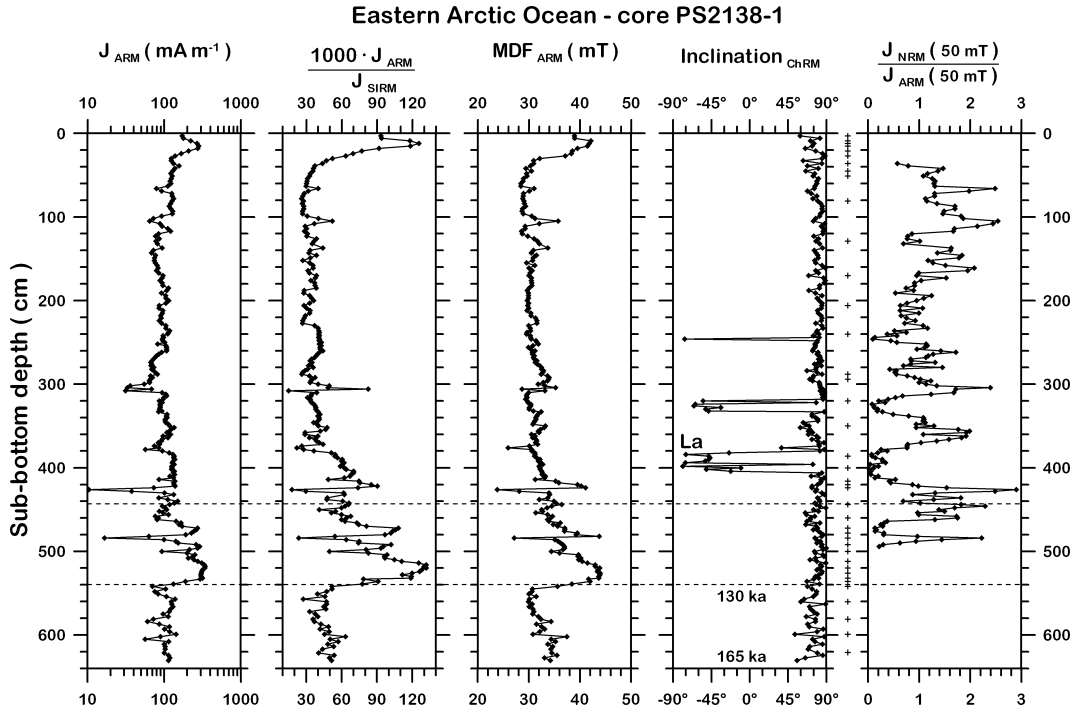


**Figure 3.** (*Continued*.)

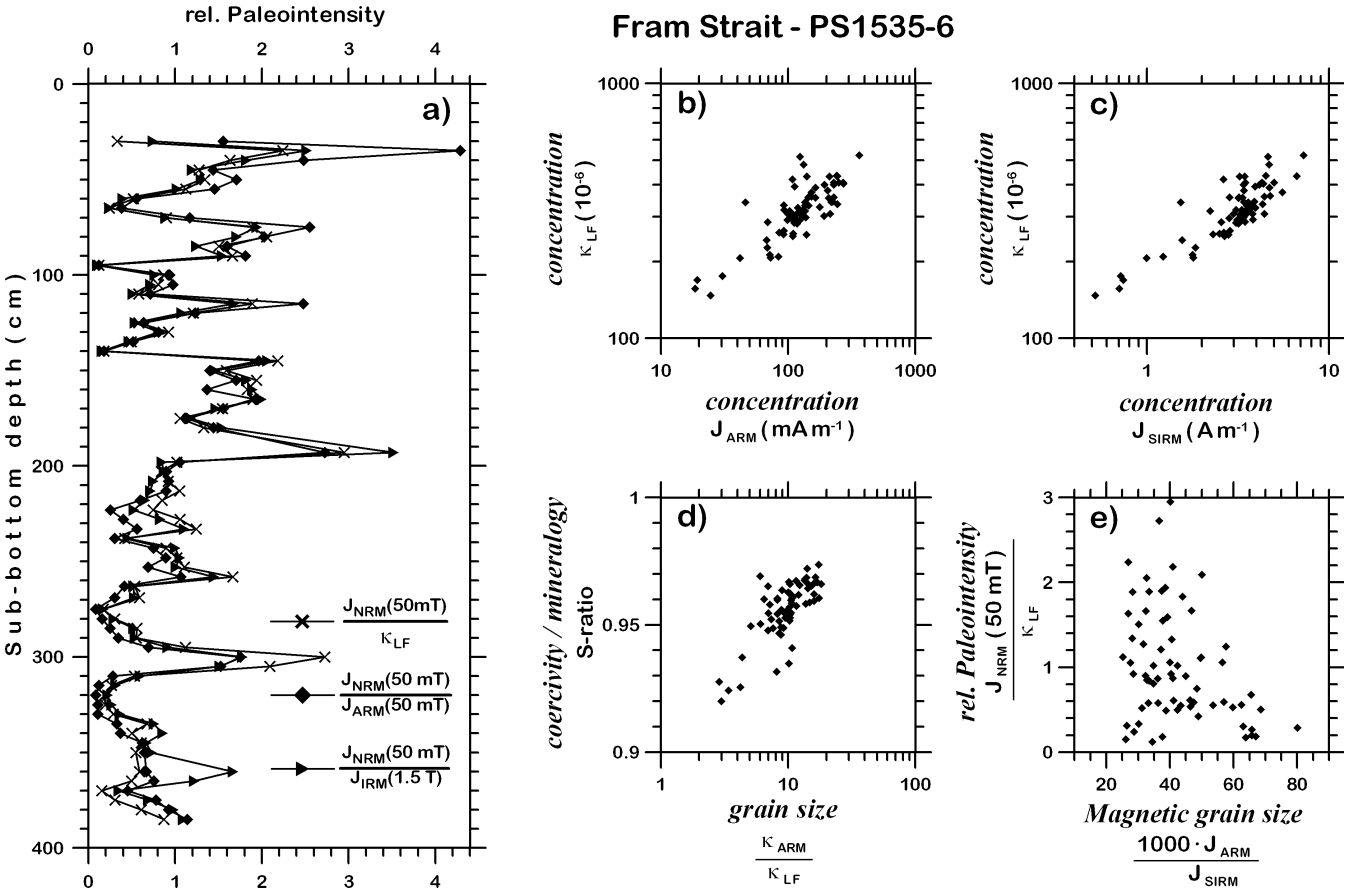


**Figure 4.** Different estimates of relative palaeointensity for core PS1535-6: (a) as indicated by the three formulae in the figure and bi-plots of concentration-related parameters with magnetic susceptibility ($\kappa_{LF}$) versus ARM intensity $J_{ARM}$ (b) and SIRM intensity $J_{SIRM}$ (c), coercivity/mineralogy ($S$-ratio) versus magnetic grain size (d), and palaeointensity estimate versus magnetic grain size (e). $S$-ratio $= 0.5 \times [1 - (IRM_{-0.3T}/SIRM_{1.5T})]$; $J_{NRM}$, intensity of natural remnant magnetization; $\kappa_{ARM}$, anhysteretic susceptibility.

Knies (2000). Core PS1535-6 shall be discussed in further detail here.

Palaeointensity estimates for all three cores based on the ratio of the intensity of the natural remnant magnetization ($J_{NRM}$) to $J_{ARM}$, both determined after alternating field demagnetization with 50 mT are displayed in the right-hand columns of Figs 3(a) and (b). In core PS1878-3 tephra layers (Nowaczyk 1997) and in core PS2138-1 the Holocene and the stage 5 sediments (Nowaczyk & Knies 2000) were not included for palaeointensity determinations. Because of the overall little to only moderate variations in concentration and grain size, sediments in core PS1535-6 are also an appropriate material for palaeointensity estimations (e.g. Tauxe 1993). Fig. 4(a) shows the three different palaeointensity estimates, $J_{NRM}/\kappa_{LF}$, $J_{NRM}/J_{ARM}$ and $J_{NRM}/J_{SIRM}$ for core PS1535-6 based on the 50 mT NRM measurement. The three average-normalized curves are of a similar morphology, that is the same succession of peaks and troughs is present in all three curves with often even the same amplitude. Since samples from the parallel cores, PS1535-8 and -10 have been used up in the meantime for other investigations, we use susceptibility-normalized palaeointensity estimates for all cores from site PS1535 instead of the preferred ARM normalization. This seems to also be justified because of a fairly linear relationship between magnetic susceptibility and ARM and SIRM intensity, respectively (Figs 4b and c). The small variations in the relatively high *S*-ratios (Fig. 4d) of 0.95 to 0.97 in core PS1535-6 (with only a few values going down to 0.92 in the lowermost part of the core equivalent to late stage 6) seem to reflect mainly grain size variations because of a rough linear correlation to log ($\kappa_{ARM}/\kappa_{LF}$), used as a grain size indicator. Finally, estimation of the relative palaeointensity ($J_{NRM}$ (50 mT)$/\kappa_{LF}$) does not show any dependence on the magnetic grain size as measured by the ratio $J_{ARM}/J_{SIRM}$ (Fig. 4e).

Besides a fairly constant magneto-mineralogy and the normalization procedure, for sediments that document reversal excursions, the correct choice of the appropriate demagnetization level is also of basic importance (Nowaczyk 1997). As mentioned earlier, sediments that carry a reversed ChRM are generally overprinted by

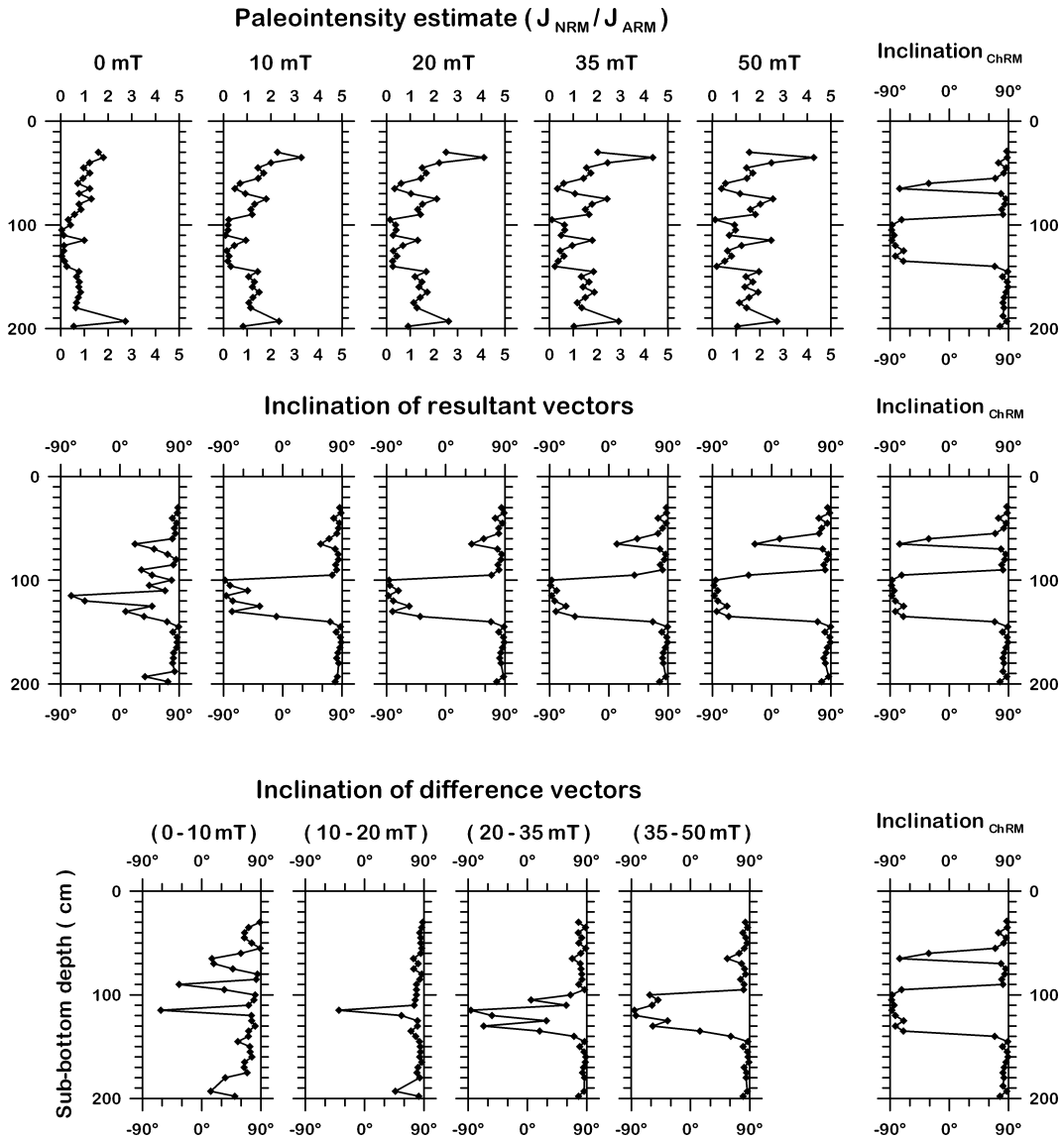


**Figure 5.** Behaviour of the relative palaeointensity estimate (here $J_{NRM}/J_{ARM}$), inclinations of resultant vectors as well as difference vectors as a function of depth and alternating field demagnetization amplitude, together with ChRM inclinations for the upper 2 m in core PS1535-6. The data clearly indicate that an AF amplitude of 50 mT is necessary in order to completely remove the influences of the normal overprint.

an antiparallel viscous component of normal polarity that had to be eliminated with up to 50 mT AF amplitude. Fig. 5 illustrates how the palaeointensity estimate (here ARM normalized) and the inclinations of resultant and difference vectors, the remanence component destroyed between two successive demagnetization steps, are changing during the demagnetization process in the upper 200 cm of core PS1535-6. At least for the Laschamp excursion between 140 and 90 cm, at first sight, a demagnetization level of 20 mT, as often used in palaeointensity studies on sediments, seems to be sufficient. However, looking at the difference vectors, it becomes obvious that solely a low-coercivity laboratory-acquired viscous component (0–10 mT), with scattered inclinations, and the normal overprint due to the recent field at the coring site (10–20 mT), with steep inclinations, are being demagnetized. Only a single sample at 115 cm is already characterized by a reversed NRM inclination. At higher levels (20–35 and 35–50 mT) the difference vector inclinations are characterized by overlapping coercivities of the normal overprint and the more AF-resistant reversed ChRM component, respectively. Finally, at higher levels the difference vectors approach the inclination values of the resultant vectors. Parallel to this, the morphologies of the palaeointensity estimates change significantly. In particular, in the interval of the Laschamp excursion, due to the progressive elimination of soft antiparallel normal overprints, the relative palaeointensity increases with higher demagnetization levels until 50 mT AF

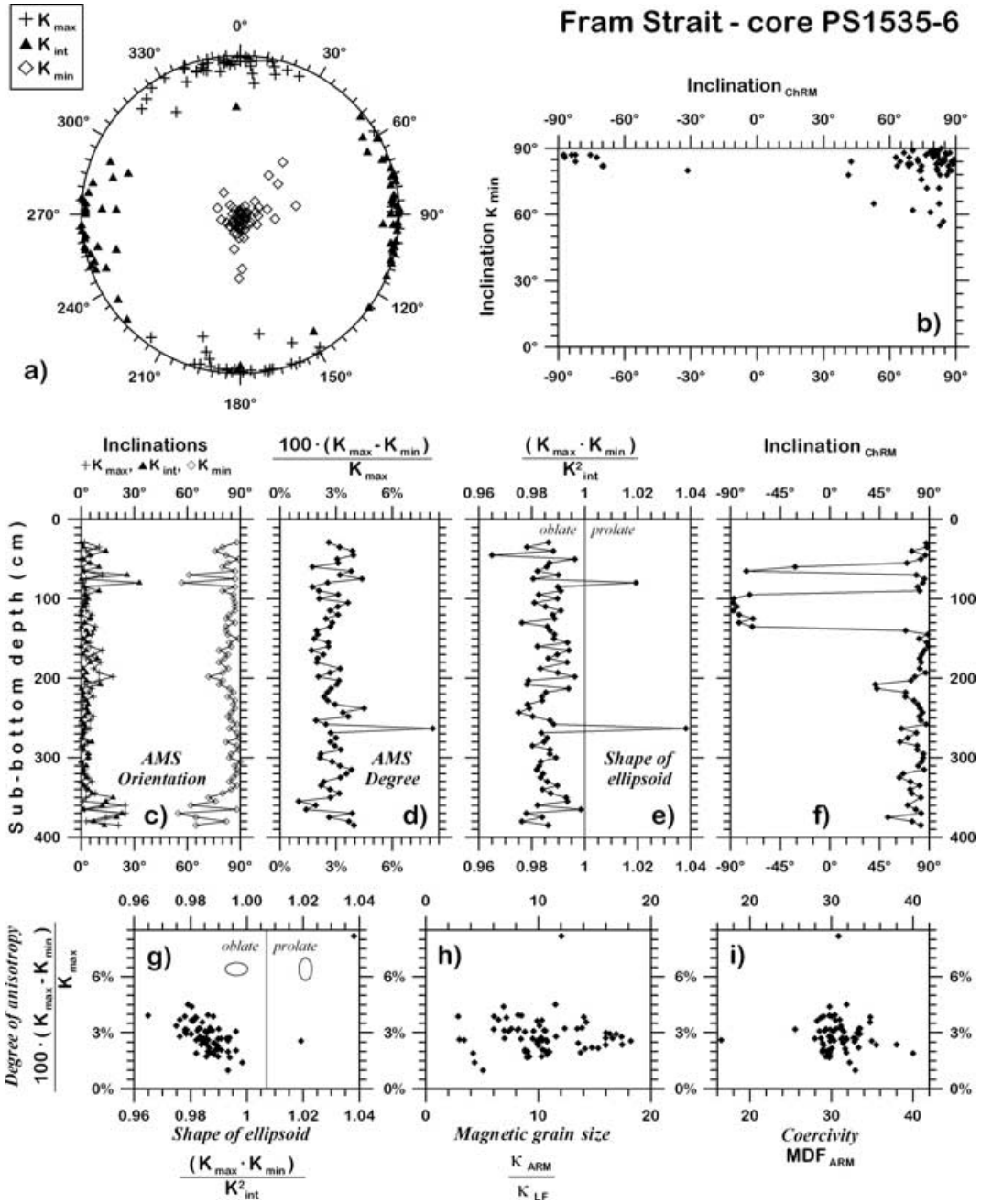


**Figure 6.** Results from determinations of the anisotropy of magnetic susceptibility performed on all samples ($n = 71$) from core PS 1535-6. (a) Orientations of the principal axes $K_{max}$, $K_{int}$ and $K_{min}$; (b) $K_{min}$ inclination versus ChRM inclination, down-core plots of principal axes (c), degree of anisotropy (d), and shape of anisotropy ellipsoid (e) compared with ChRM inclination (f), degree of anisotropy versus shape of anisotropy (g), magnetic grain size (h) and coercivity (i).

level. Consequently, as in previous studies, we used this demagnetization level of the NRM for estimation of relative palaeointensity variations.

Results from determination of the anisotropy of the magnetic susceptibility (Fig. 6) indicate that, in most cases, the investigated sediments are characterized by an oblate ellipsoid ($K_{max} \times K_{min}/K_{int}^2 < 1$) with the ellipsoid being flatter when anisotropy is high (Fig. 6g). The degree of anisotropy ($100 \times (K_{max} - K_{min})/K_{max}$) is relatively low (Fig. 6d), ranging only between 2 and 4 per cent. The small principal axis $K_{min}$ is oriented perpendicular to the bedding plane (Figs 6a, c and e) with $K_{min}$ inclinations mainly between 80° and 90°. Principal axes $K_{int}$ and $K_{max}$ are nearly of the same length: mean $K_{int} \approx 1.005$, mean $K_{max} \approx 1.010$, with mean $K_{min} \approx 0.980$ (Nowaczyk 2003; Fig. 3a). $K_{int}$ and $K_{max}$ are oriented horizontally (Fig. 6a) with an apparent alignment parallel to the *x*-axis = 0°/180°($K_{max}$) and the *y*-axis = 90°/270°($K_{int}$). However, the centres of their distributions are rotated by approximately −10°. The difference between $K_{int}$ and $K_{max}$ is just 0.5 per cent. The mean bulk susceptibility is approximately $300 \times 10^{-6}$, so that the difference between $K_{int}$ and $K_{max}$ is just $1.5 \times 10^{-6}$ in absolute values. We therefore suspect that the preferred alignment of $K_{int}$ and $K_{max}$ could be a numerical artefact of the applied software, especially because other cores with higher degrees of anisotropy do not show a preferred alignment such as in core PS1535-6 (Nowaczyk 2003). Anisotropy parameters of core PS1535-6 are quite constant over the whole core, and ChRM inclinations (Fig. 6f) neither show any relationship to the orientation of the principal axes of the anisotropy ellipsoid (Figs 6b and c), nor to the degree (Fig. 6d), nor to the shape of the anisotropy ellipsoid (Fig. 6e). The degree of anisotropy is also independent of the magnetic grain size (Fig. 6h), as measured by the susceptibility ratio $\kappa_{ARM}/\kappa_{LF}$, and independent of coercivity (Fig. 6i), as measured by the median destructive field of the ARM ($MDF_{ARM}$). In summary, it can be concluded that reversed inclinations at site PS1535-6 are expressions of geomagnetic field variations and not artefacts, because, both bulk rock magnetic parameters as well as the magnetic fabric do not change across the boundaries of directional variations (Figs 3–6).

In core PS1535-6, *S*-ratios mainly between 0.95 and 0.97 (Fig. 4d), indicate that (titano-)magnetite should be the dominant magnetic mineral. In order to further clarify this point, 67 low-temperature measurements of magnetic susceptibility were performed. The results from 24 representative samples, six (out of 17)

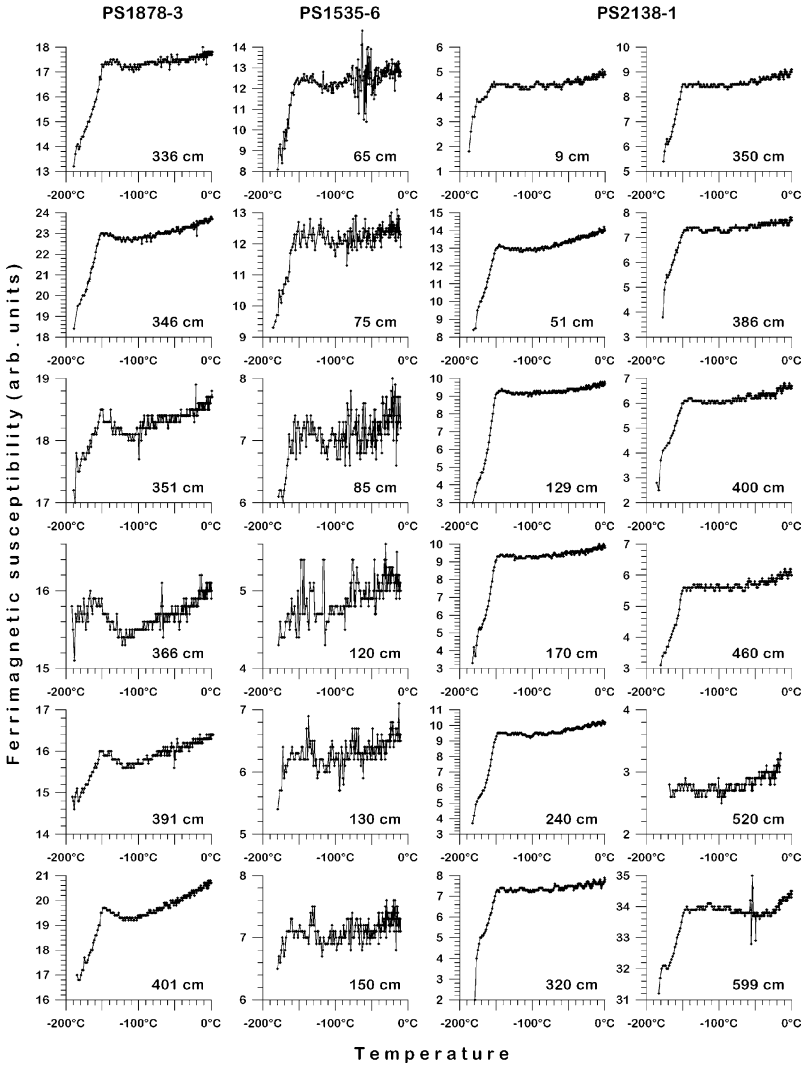


**Figure 7.** Ferrimagnetic susceptibility during low-temperature measurements of samples from cores PS1878-3 (six out of 17), PS1535-6 (six out of 10) and PS2138-1 (12 out of 40). The data are shown after separation of ferrimagnetic from paramagnetic susceptibility with the procedure as described in the text (see also Nowaczyk *et al.* 2002).

from core PS1878-3, Greenland Sea, six (out of 10) from core PS1535-6, Fram Strait and 12 (out of 40) from core PS2138-1, Eastern Arctic Ocean, after separation of the ferrimagnetic susceptibility, are shown in Fig. 7. The positions of all measured samples are marked by small crosses between the ChRM inclination records and the palaeointensity estimates shown in Figs 3(a) and (b). The frequent presence of the Verwey transition, that is, a significant increase of magnetic susceptibility until −150 °C and a subsequent plateau during warming up of the samples indicates that even pure magnetite is the dominant magnetic mineral in nearly all investigated samples of the three sites. This is supported by further rock magnetic investigations of core PS1535-8 (Frederichs 1995).

### Dating

Complete age–depth relationships for the three investigated cores are shown in Fig. 8. Age determinations were derived from nanofossil biostratigraphy (PS1535-8), dinoflagellate cyst stratigraphy (PS1535-8, PS2138-1), oxygen isotope stratigraphy (PS1535-8, PS1878-3, PS2138-1), and correlation to palaeointensity reference curves (PS1535stack, PS2138-1), respectively. In addition, a total of 44 AMS $^{14}$C ages (Table 2) are now available for the three cores which, in general, confirm the older age models.

Based on a correlation using magnetic susceptibility, ChRM inclination, and relative palaeointensity data from the three Fram Strait cores 1535-6, -8, and -10 a composite record for site PS1535 with respect to the depth scale of core PS1535-8 for the upper 300 cm was created. The data sets, ChRM inclination and relative palaeointensity, were recalculated (interpolated) to 1 cm intervals and then stacked. In this stack, between 200 and 300 cm composite depth, approximately equivalent to the younger part of oxygen isotope stage 5 (back to 105 ka), two older excursions at approximately 72 ka, 'Norwegian–Greenland Sea' and 98 ka, 'Fram Strait', are visible (Fig. 3a). They have already been discussed in detail by Nowaczyk & Baumann (1992). A similar stack of palaeomagnetic data has been created for the Greenland Sea sites PS1707-2, PS1878-3, PS1882-2 and PS1892-3, with data from Nowaczyk & Antonow (1997) and Nowaczyk (1997). The palaeointensity stacks from the Greenland Sea and the Fram Strait, together with palaeointensity data from site PS2138-1 are compared with data from ODP site 983 (Channell *et al.* 1997, fig. 1), Iceland Sea in Fig. 9. Dotted lines mark the positions of excursions younger than 50 ka. There is a general agreement between the four curves in the way that the documented excursions are dated at similar ages and that they all are clearly associated with lows in relative palaeointensity. However, the database is quite heterogeneous in terms of variable data density. This different temporal resolution is caused by different sedimentation rates (Fig. 8), but also by different sample spacing (centre-to-centre: 2–3 cm in PS2138-1 and 5 cm at sites PS1535 and PS1878).

Fig. 10(a) focuses on the time interval from approximately 15 ka back to shortly before the Laschamp reversal excursion, showing palaeomagnetic results, ChRM inclinations and relative palaeointensities, dated by accelerator mass spectrometry $^{14}$C dating. Dashed curves in plots for site PS1535 mark the maximum and minimum deviation of the individual records from the respective stacks. In Fig. 10(b), which gives a more detailed image of the results, focusing further only on the Laschamp excursion, the individual data are plotted together with the stacks from site PS1535.

## DISCUSSION

In order to check whether the three sites yielded consistent AMS $^{14}$C results at all, and in order to avoid artificial biases by tuning

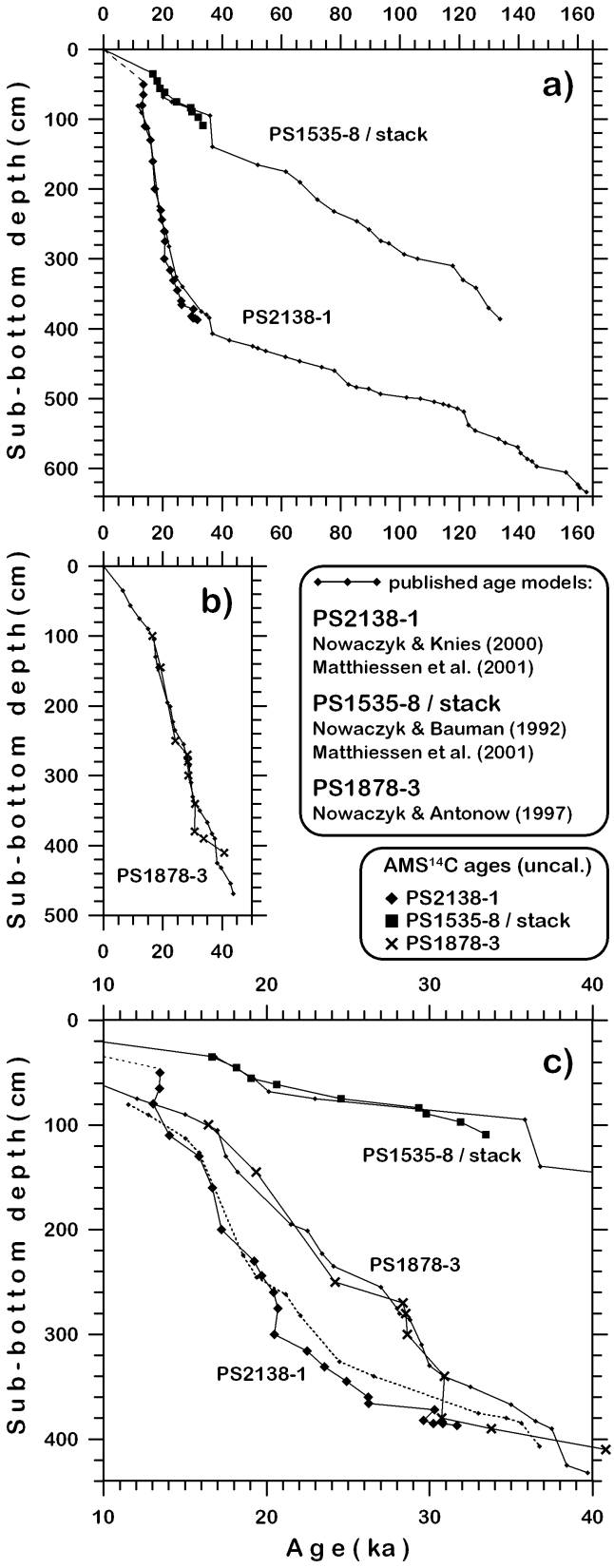


**Figure 8.** Age–depth relationships for the cores PS1535-8/stack and PS2138-1 (a) and PS1878-3 (b) with age models referenced in the legend. The lower graph displays the age models with expanded axes for the time window covered by accelerator mass spectrometry (AMS) $^{14}$C age determinations (c).

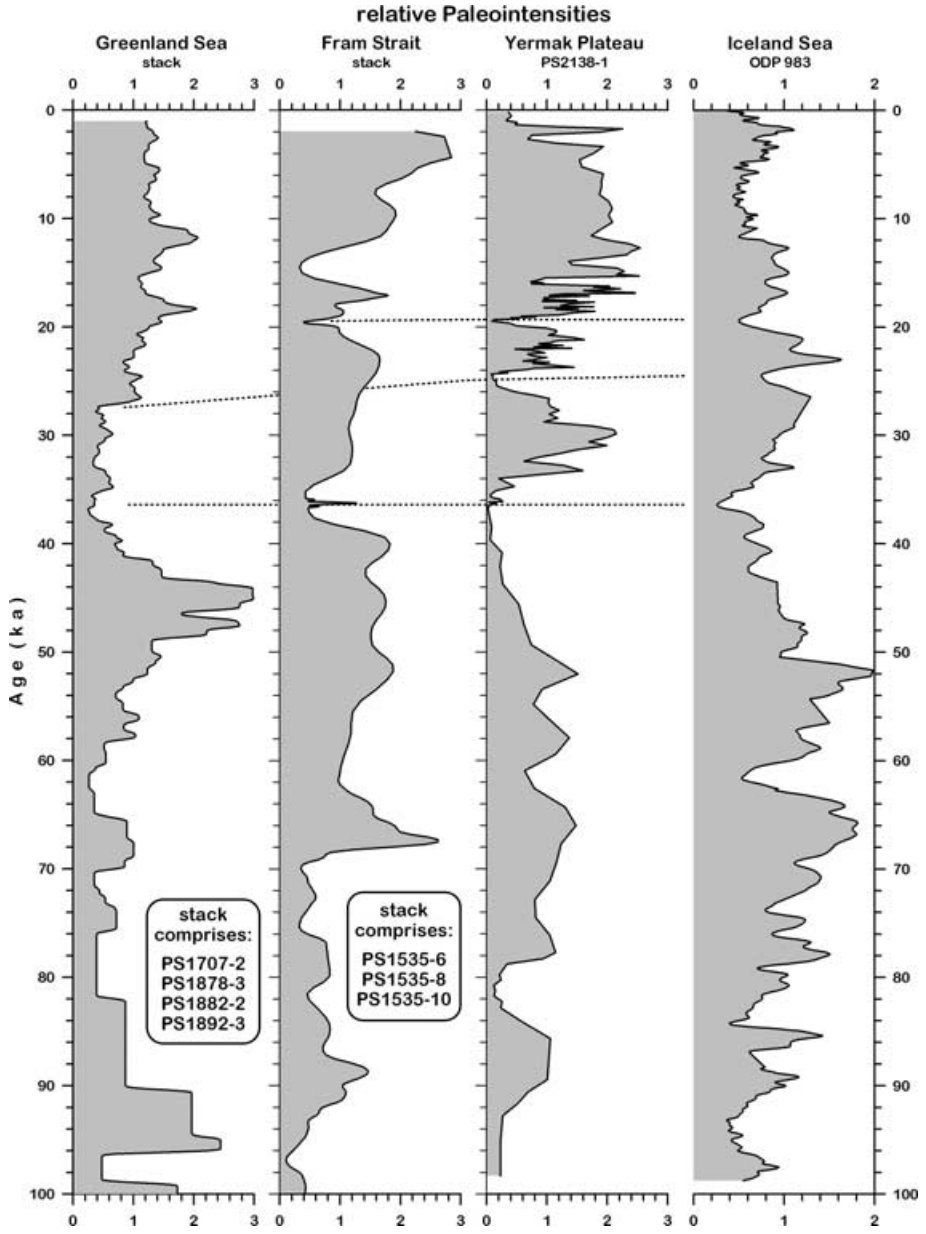


**Figure 9.** Relative palaeointensities from Greenland Sea, Fram Strait and Yermak Plateau compared with the Iceland Sea record from ODP site 983 (Channell *et al.* 1997).

the records to other non-palaeomagnetic records, we discuss the obtained dating on the basis of uncalibrated ages. However, we also gave the calibrated ages in Table 2.

At all three sites the termination of the Laschamp excursion is quite consistently dated to be at 30–31 ka (uncalibrated AMS $^{14}$C), probably with the most unproblematic dating results in core PS1535-8. Generally, there are some problems in the obtained age data marked by question marks. In core PS2138-1, three samples, 372, 375 and 380 cm, from sediments deposited after the termination of the Laschamp excursion at 381 cm yielded AMS $^{14}$C ages older than the termination of the excursion, whereas two samples from core PS1878-3, 370 and 380 cm, from within the Laschamp excursion yielded ages younger than the termination of the excursion at 350 cm. Nevertheless, the onset of the excursion seems to be reliably dated in core PS1878-3 to be at approximately 34 ka. Taking all three cores together, a total duration of 3–4 ka on the uncalibrated $^{14}$C timescale can be estimated.

One very short excursion is centred at 20 ka (uncalibrated) in core PS2138-1 (Nowaczyk & Knies 2000) and in all three cores from site PS1535 (Figs 9 and 10). This excursion in cores from site PS1535 first was related to the Mono Lake excursion (Denham & Cox 1971; Liddicoat & Coe 1979) by Nowaczyk & Baumann (1992), but obviously it is clearly younger than that. So, according to Nowaczyk & Knies (2000), this should be looked upon as an additional excursion. Evidence for two subsequent excursions following the Laschamp excursion may also come from volcanic rocks drilled on Hawaii (Laj *et al.* 2002). Between this short-term feature and the Laschamp excursion an excursion is documented at around 23 ka in

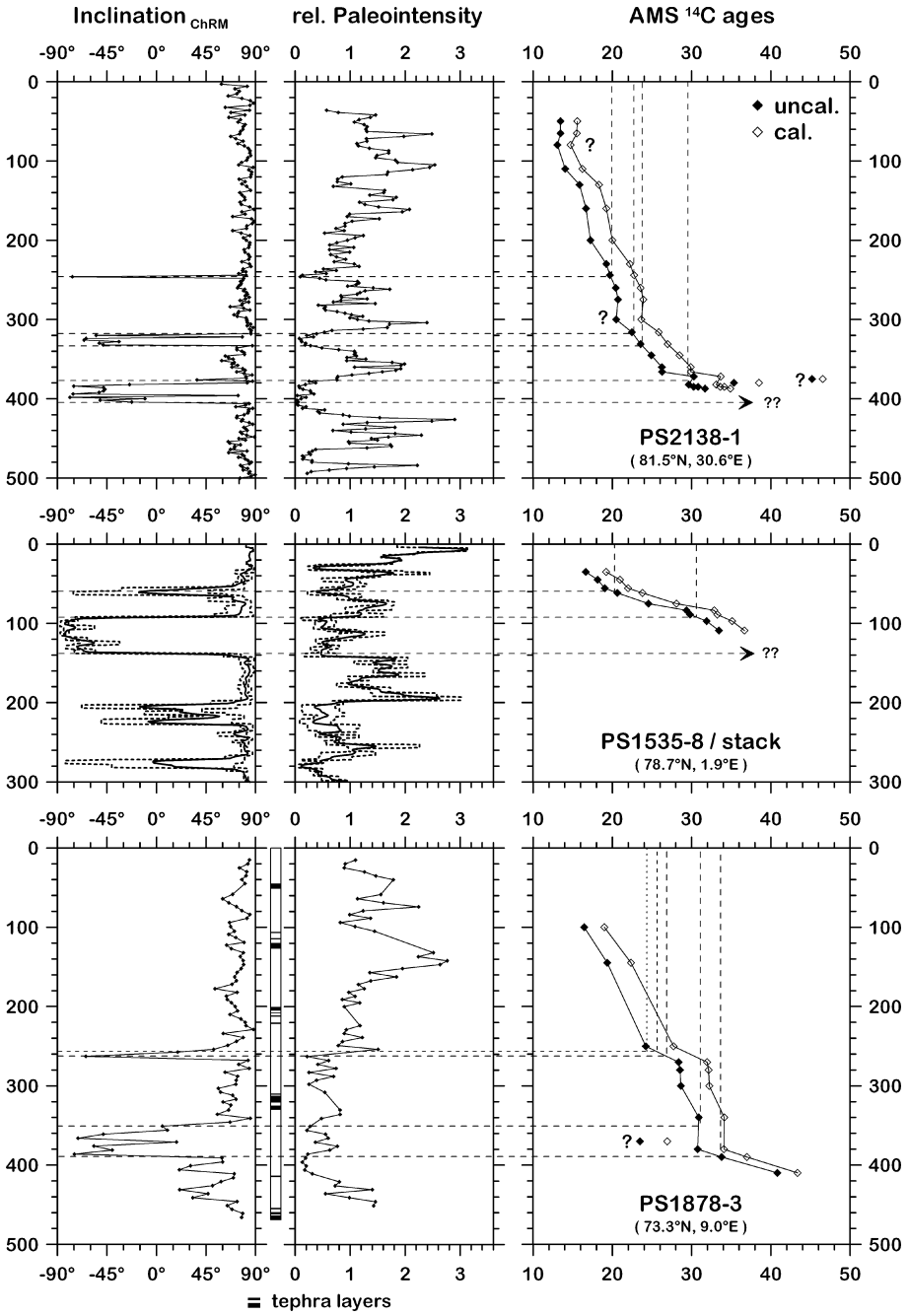


**Figure 10.** (a) Compilation of ChRM inclinations, relative palaeointensity estimates and accelerator mass spectrometry (AMS) $^{14}$C ages, uncalibrated (filled diamonds) as well as calibrated (open diamonds) for the three high-latitude sites discussed in this paper. Question marks indicate uncertainties in age determinations. The simplified lithology log of PS1878-3 indicate positions of tephra layers (see Nowaczyk 1997). Question marks indicate problematic dating results. (b) Same as (a) but with a focus on the Laschamp event. Filled diamonds in the stacked palaeomagnetic records of site PS1535 mark the results of the three individual cores used for the stack. Dotted lines indicate clear age assignments, whereas (widely) dashed lines indicate less certain (questionable) age assignments.

core PS2138-1 and at around 25 ka in core PS1878-3, respectively, which is thus more probably a documentation of the Mono Lake excursion.

Both, onset and termination of the Laschamp excursion, as well as the two subsequent excursions, are linked with the lowest palaeointensity estimates. However, unlike in other published records, e.g. Channell *et al.* (1997), Laj *et al.* (2000), a significant field recovery during the reversed state of the Laschamp excursion, approximately threefold when compared with the minima of the N–R and R–N transitions, is documented in this high-resolution study, with a thickness of sediments with excursional directions of up to 45 cm. This small but significant field recovery makes the Laschamp excursion appear a little bit like a real reversal event, e.g. such as the Jaramillo event within the Matuyama Chron, but with a much shorter duration. The missing of this field recovery in other studies might be due to the applied u-channel technique (e.g. Channell *et al.* 2000; Laj *et al.*

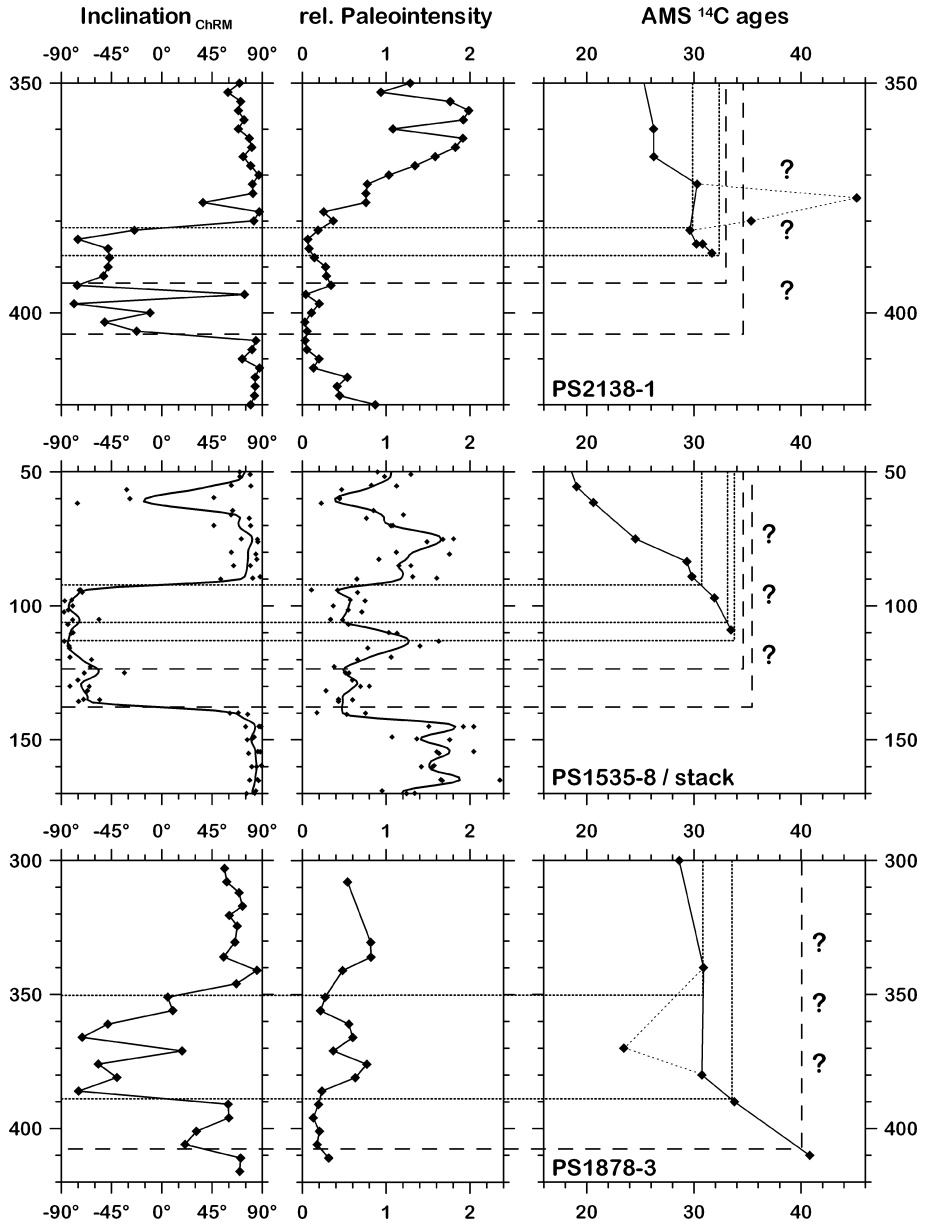


**Figure 10.** (*Continued*.)

2000) which generally suffer more or less from smoothing due to the broad sensor characteristics of the whole-core magnetometers. In addition, palaeointensity estimates are frequently determined on demagnetization levels of 20–30 mT. This is, at least in the case of Arctic marine sediments, definitely too low in order to really resolve the palaeointensity variations in very great detail, that is, completely eliminate the often antiparallel viscous overprints of normal polarity from the stable reversed directions (see Fig. 5 and Nowaczyk & Antonow 1997).

Probably the palaeomagnetic records from site PS1535 (Figs 10a and b) with the best temporal resolution indicate a three-phase structure of the Laschamp excursion at northern high latitudes. The second (middle) phase is associated with the highest relative palaeointensities and the steepest negative inclinations of $-80^\circ$ to $-90^\circ$, whereas the first and third phases, including the N–R and R–N transitions, respectively, are characterized by the lowest relative palaeointensities across the excursion. In addition, the first phase is linked with significantly lower ChRM inclinations, mostly between $-50^\circ$ and $-80^\circ$. A similar structure, but less well established, is also visible in the records of cores PS2138-1 and PS1878-3 (Fig. 10b). The maximum of the field recovery is dated at approximately 31.5 ka at site PS1535, so that approximately the second half of the excursion would have a duration of approximately 1.5 ka on an uncalibrated $^{14}$C timescale. Unfortunately, paleomagnetic data and AMS $^{14}$C ages from PS1878-3 are too sparse to cross-check these findings.

The generally low field intensities associated with the Laschamp reversal excursion caused a largely increased production of cosmogenic isotopes, such as $^{10}$Be (McHargue *et al.* 1995, 2000), $^{36}$Cl (Wagner *et al.* 2000), and of course $^{14}$C (Voelker *et al.* 1998). In general, this complicates the interpretation of AMS $^{14}$C ages, since the calibration to calendar ages is then not straightforward. Voelker *et al.* (1998) attempted to obtain a solution of this problem from another site in the Iceland Sea. A relative large number of AMS $^{14}$C datings (Fig. 11) was performed on core PS2644-5 from 67.9°N

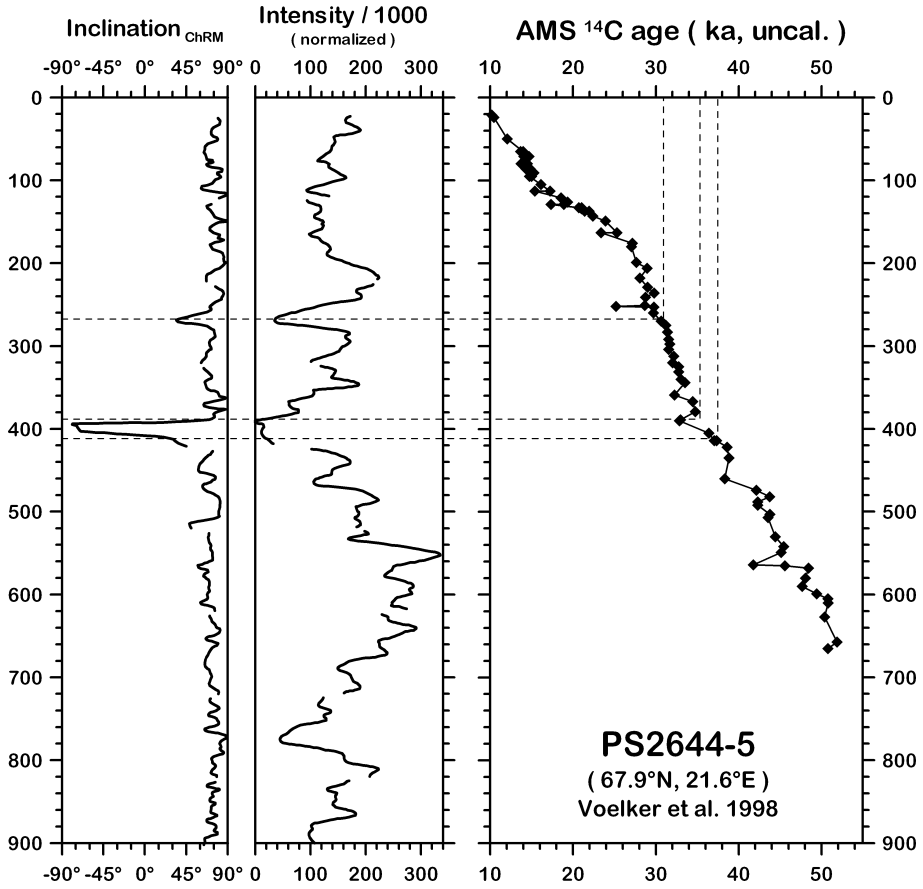


**Figure 11.** ChRM inclination, relative palaeointensity and AMS $^{14}$C ages from core PS2644-5, Iceland Sea Greenland (after Voelker *et al.* 1998).

(Fig. 1), reaching back to approximately 50 ka (uncalibrated). However, magneto-chronostratigraphic results from this core (Voelker *et al.* 1998) are in some contrast to the quite consistent results from the three sites from 73.3°N to 81.5°N. When comparing the polarity patterns derived from the cores of this study to core PS2644-5 (Fig. 12) there seems to be an offset for both the Laschamp and the Mono Lake excursion to younger ages by approximately 4 ka.

All four sites spread over a distance of roughly 2000 km (Fig. 1). The distance between sites PS2644 and PS1878, with diverging ages, is approximately 550 km. This is quite small when compared with the distance from (≥3000 km) and to the diameter of the geodynamo (approximately 7000 km), the source of the geomagnetic field within the Earth's outer core. Moreover, data from sites PS1878, PS1535 and PS2138, which span across a distance of approximately 1500 km, are relatively consistent both in terms of dating and paleomagnetic results. Thus, it can be excluded that time transgressive processes associated with the excursional process could be responsible for the apparently different timing of the Laschamp excursion

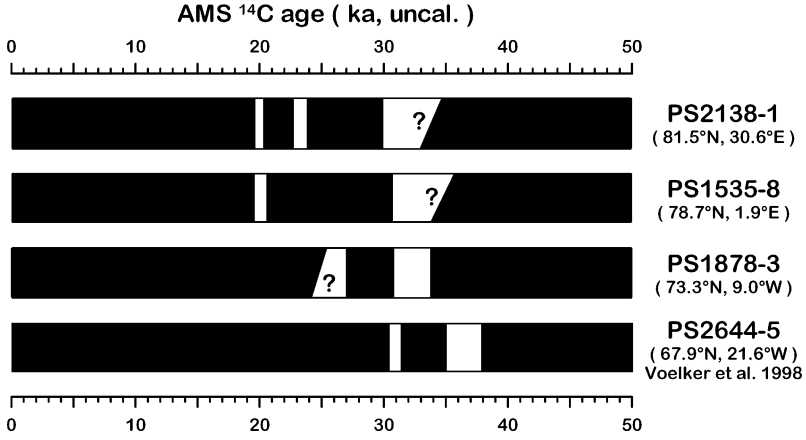


**Figure 12.** Polarity patterns of the four cores shown in Figs 10(a) and (b), and Fig. 11 as a function of uncalibrated AMS $^{14}$C age, with black indicating normal and white indicating reversed polarity. Question marks and inclined boundaries of the white fields indicate uncertain ages of the boundaries of the excursions.

at the southernmost site, when compared with the other three sites further north. An explanation of the divergences by different lock-in times related to a post-depositional DRM, which then must be of the order of 5000 yr, is unrealistic, because at least at sites PS2644, PS1878 and PS2138 sedimentation rates are of the same magnitude and sediments at all of these sites are characterized by a similar lithology. Largely differing pDRM processes thus can also be excluded as an explanation.

All four cores have been dated in the same AMS facility (Kiel, Germany) using similar material (in general foraminiferes of the same species). Systematic errors in dating between the four cores yielding significant age shifts can be excluded (Grootes, AMS facilities Kiel, pers. comm. 2002) The different paleomagnetic processing techniques (Voelker *et al.* 1998, u-channels; this study, discrete samples) should not play a major role since this should normally result just in a different frequency content of the data but not in time-shifts.

One more likely explanation might be that different reservoir ages are responsible for the dating divergences. Sedimentation at sites PS1878, PS1535 and PS2138 was more influenced by open water conditions than at site PS2644. In particular, site PS2138 was obviously influenced by a Polynia, open water conditions due to strong winds keeping the sea water free from ice (Nowaczyk & Knies 2000). This enabled growth of foraminifers and, much more importantly, a more or less direct exchange of atmospheric gases with sea water, that is, the ocean and the atmosphere were in equilibrium. In contrast to this, site PS2644 is more influenced by conditions characterized by more or less severe ice covering, inhibiting a direct gas exchange between the atmosphere and the sea water. This in turn should have resulted in much higher reservoir ages (Grootes, AMS facilities Kiel, pers. comm. 2002). An additional, or possibly alternative explanation could be that at site PS2644 much more continental glacier ice from Greenland is expelled to the sea, e.g. through the Scoresby Sound, when compared with the sites further north and further offshore from Greenland. This old glacial ice should carry a lot of old $CO_2$ depleted in $^{14}$C. After melting of the icebergs and mixing with sea water, the $^{14}$C content of the water is lower than the $^{14}$C content of the atmosphere. The old $CO_2$ was then incorporated by the foraminifers, yielding apparently older ages.

In summary, all available chronological information, although of high quality in terms of technical precision, do not yield a consistent image of the geomagnetic variations throughout the last 50 ka. Differences in 'absolute' dating of the geomagnetic features by the accelerator mass spectrometry technique of sediments from the four sites must be due to different reservoir ages and/or mixing with old $CO_2$ from glaciers. Unfortunately up to now, no other records have been available which could supply both high-quality palaeomagnetic data and a sufficient number of AMS $^{14}$C datings that could help in resolving the problems in precisely dating the three youngest excursions of the geomagnetic field.

## CONCLUSIONS

During the last 50 ka the geomagnetic field very likely went into three crises which were characterized by pronounced decreases of its intensity by more than an order of magnitude compared with the field maximum at around 50 ka. These decays in intensity were associated with a complete geomagnetic reversal at least of the regional field vector in the area of the Norwegian–Greenland Sea and the eastern Arctic Ocean. The most pronounced geomagnetic feature in this time window is the Laschamp excursion which exhibits features such as longer polarity events, that is, lowest relative palaeointensities were found at the N–R and R–N transitions with a significant field recovery for a short time between the transitions. This behaviour was found at all three sites investigated. The Laschamp excursion was followed by the Mono Lake excursion and probably a second even shorter excursion. However, absolute dating of these three excursions is still a problem. AMS $^{14}$C dating performed on the same type of material (foraminifers) processed at the same AMS facility (Kiel, Germany) still yielded diverging results when including additional data from literature for a fourth site further to the southwest (PS2644-5). Ages for the Laschamp and Mono Lake excursion, respectively, are older by approximately 4 ka here. Possibly, these diverging ages could be explained by a strong reservoir effect due to a larger ice cover, when compared with the other sites, and/or by a mixing of old $^{14}$C-depleted $CO_2$ from glaciers with sea water. Thus there is a need for more detailed investigations focusing both on AMS $^{14}$C dating, including a precise estimation of reservoir ages and 'contamination' with old $CO_2$, and exact determination of palaeomagnetic directions and relative palaeointensities. In addition, other independent stratigraphic tools must be applied in order to synchronize palaeomagnetic data and AMS $^{14}$C chronologies.

## ACKNOWLEDGMENTS

The crews of RV Polarstern are acknowledged for their technical support during cruises ARK IV/3, ARK VII/1 and ARK VIII/2. The Alfred-Wegener-Institut für Polar- und Meeresforschung provided shiptime. R. Volkman helped to pick the forams for AMS dating. This is a contribution to the priority programme '*Geomagnetic variations: variation in time and space, processes and impact on the system Earth*', of the Deutsche Forschungsgemeinschaft (German science foundation).

## REFERENCES

Bleil, U., 1989. Magnetostratigraphy of Neogene and Quaternary sediment series from the Norwegian Sea: Ocean Drilling Program, Leg 104, *Proc. Ocean Drill. Progr., Sci. Res.,* **104,** 829–850.

Bleil, U. & Gard, G., 1989. Chronology and correlation of Quaternary magnetostratigraphy and nanofossil biostratigraphy in Norwegian–Greenland Sea sediments, *Geol. Rundschau,* **78,** 1173–1187.

Bonhommet, N. & Babkine, J., 1967. Sur la présence d'aimantations inversées dans la Chaîne des Puys, *C.R. Acad. Sci. Paris,* **264,** 92–94.

Channell, J.E.T., Hodell, D.A. & Lehman, B., 1997. Relative geomagnetic paleointensity and $\delta^{18}$O at ODP Site 983 (Gardar Rift, North Atlantic) since 350 ka, *Earth planet. Sci. Lett.,* **153,** 103–118.

Channell, J.E.T., Stoner, J.S., Hodell, D.A. & Charles, C.D., 2000. Geomagnetic paleointensity for the last 100 kyr from the sub-Antarctic South Atlantic: a tool for inter-hemispheric correlation, *Earth planet. Sci. Lett.,* **175,** 145–160.

Denham, C.R. & Cox, A., 1971. Evidence that the Laschamp polarity event did not occur 13 300–30 400 years ago, *Earth planet. Sci. Lett.,* **13,** 181–190.

Frederichs, T., 1995. Regional and temporal variations of rock magnetic parameters in Arctic marine sediments, *Dissertation,* University of Bremen (in German with English abstract), *Rep. PolarRes.,* **164,** 212.

Gillot, P.Y., Labeyrie, J., Laj, C., Valladas, G., Guérin, G., Poupeau, G. & Delibrias, G., 1979. Age of the Laschamp paleomagnetic excursion revisited, *Earth planet. Sci. Lett.,* **42,** 444–450.

Kirschvink, J.L., 1980. The least-squares line and plane and the analysis of palaeomagnetic data, *Geophys. J. R. astr. Soc.,* **62,** 699–718.

Knies, J., Nowaczyk, N., Müuller, C., Stein, R. & Vogt, C., 2000. A multiproxy approach to reconstruct the environmental changes along the Eurasian continental margin over the last 150 000 years, *Mar. Geol.,* **163,** 317–344.

Laj, C., Kissel, C., Mazaud, A., Channell, J.E.T. & Beer, J., 2000. North Atlantic palaeointensity stack since 75 ka (NAPIS75) and the duration of the Laschamp event, *Phil. Trans. R. Soc. Lond. A,* **358,** 1009–1025.

Laj, C., Kissel, C., Scao, V., Beer, J., Thomas, D.M., Guillou, H., Muscheler, R. & Wagner, G., 2002. Geomagnetic intensity and inclination variations at Hawaii for the past 98 kyr from core SOH-4 (Big Island): a new study and a comparison with existing contemporary data, *Phys. Earth planet. Inter.,* **129,** 205–243.

Levi, S., Audunsson, H., Duncan, R.A., Kristjansson, L., Gillot, P.-Y. & Jacobsson, S.P., 1990. Late Pleistocene geomagnetic excursion in Icelandic lavas: confirmation of the Laschamp excursion, *Earth planet. Sci. Lett.,* **96,** 443–457.

Liddicoat, J.C. & Coe, R.S., 1979. Mono Lake geomagnetic excursion, *J. geophys. Res.,* **84B,** 261–271.

Løvlie, R., Markussen, B., Sejrup, H.P. & Thiede, J., 1986. Magnetostratigraphy in three Arctic Ocean sediment cores; arguments for geomagnetic excursions within oxygen-isotope stage 2–3, *Phys. Earth planet. Inter.,* **43,** 173–184.

McHargue, L.R., Damon, P.E. & Donahue, D.J., 1995. Enhanced cosmic-ray production of $^{10}$Be coincident with the Mono Lake and Laschamp geomagnetic excursions, *Geophys. Res. Lett.,* **22**(5), 659–662.

McHargue, L.R., Donahue, D., Damon, P.E., Sonett, C.P., Biddulph, D. & Burr, G., 2000. Geomagnetic modulation of the late Pleistocene cosmic-ray flux as determined by $^{10}$Be from Blake Outer Ridge marine sediments, *Nucl. Instr. Meth. Phys. Res.,* **172B,** 555–561.

Matthiessen, J., Knies, J., Nowaczyk, N.R. & Stein, R., 2001. Late Quaternary dinoflagellate cyst stratigraphy at the Eurasian continental margin, Arctic Ocean: indications for Atlantic water inflow in the past 150 000 years, *Global Planet. Change,* **31,** 65–86.

Nowaczyk, N.R., 1997. High-resolution magnetostratigraphy of four sediment cores from the Greenland Sea II—rock magnetic and paleointensity data, *Geophys. J. Int.,* **131,** 325–334.

Nowaczyk, N.R., 2003. Detailed study on the anisotropy of magnetic susceptibility of arctic marine sediments, *Geophys. J. Int.,* **152,** 302–317.

Nowaczyk, N.R. & Antonow, M., 1997. High-resolution magnetostratigraphy of four sediment cores from the Greenland Sea I—Identification of the Mono Lake excursion, Laschamp and Biwa I/Jamaica geomagnetic polarity events, *Geophys. J. Int.,* **131,** 310–324.

Nowaczyk, N.R. & Baumann, M., 1992. Combined high-resolution magnetostratigraphy and nanofossil biostratigraphy for Late Quaternary Arctic Ocean sediments, *Deep-Sea Res.,* **39,** 567–601.

Nowaczyk, N.R. & Frederichs, T.W., 1999. Geomagnetic events and relative paleointensity variations during the last 300 ka as recorded in Kolbeinsey Ridge Sediments, Iceland Sea—indication for a strongly variable geomagnetic field, *Int. J. Earth Sci.,* **88,** 116–131.

Nowaczyk, N.R. & Knies, J., 2000. Magnetostratigraphic results from Eastern Arctic Ocean—AMS $^{14}$C ages and relative palaeointensity data of the Mono Lake and Laschamp geomagnetic reversal excursions, *Geophys. J. Int.,* **140,** 185–197.

Nowaczyk, N.R., Frederichs, T.W., Eisenhauer, A. & Gard, G., 1994. Magnetostratigraphic data from Late Quaternary sediments from the Yermak Plateau, Arctic Ocean: evidence for four geomagnetic polarity events within the last 170 ka of the Brunhes Chron, *Geophys. J. Int.,* **117,** 453–471.

Nowaczyk, N.R., Frederichs, T.W., Kassens, H., Nørgaard-Pedersen, N., Spielhagen, R.F., Stein, R. & Weiel, D., 2001. Sedimentation rates in the Makarov Basin, Central Arctic Ocean—a paleo- and rock magnetic approach, *Paleoceanography,* **16**(4), 368–389.

Nowaczyk, N.R. *et al.,* 2002. Magnetostratigraphic results from impact crater Lake El'gygytgyn, northeastern Siberia: a 300 kyr long high-resolution terrestrial palaeoclimatic record from the Arctic., *Geophys. J. Int.,* **140,** 109–126.

Schneider, D.A., Backman, J.M.F., Curry, W.B & Possnert, G., 1996. Paleomagnetic constraints on sedimentation rates in the eastern Arctic Ocean, *Quat. Res.,* **46,** 62–71.

Stuiver, M. & Reimer, P.J., 1993. Extended 14C database and revised CALIB radiocarbon calibration program, *Radiocarbon,* **35,** 215–230.

Stuiver, M. *et al.,* 1998. INTCAL98 radiocarbon age calibration, 24 000–cal BP, *Radiocarbon,* **40**(3), 1041–1083.

Tauxe, L., 1993. Sedimentary records of relative paleointensity of the geomagnetic field: theory and practice, *Rev. Geophys.*, **31,** 319–354.

Vlag, P., Thouveny, N., Williamson, D., Rochette, P. & Ben-Atig, F., 1996. Evidence for a geomagnetic excursion recorded in the sediments of Lac St Front, France: a link with the Laschamp excursion?, *J. geophys. Res.,* **101**(B12), 28 211–28 230.

Voelker, A.H.L., Sarnthein, M., Grootes, P.M., Erlenkeuser, H., Laj, C., Mazaud, A., Nadeau, M.-J. & Schleicher, M., 1998. Correlation of marine $^{14}$C ages from the Nordic Seas with the GISP2 isotope record: implications for $^{14}$C calibration beyond 25 ka, *Radiocarbon,* **40,** 517–534.

Wagner, G., Beer, J., Laj, C., Kissel, C., Masarik, J., Muscheler, R. & Synal, H.-A., 2000. Chlorine-36 evidence for the Mono Lake event in the Summit GRIP ice core, *Earth planet. Sci. Lett.,* **181,** 1–6.